This ESI replaces the original version published on 03 Jan 2025.

**Nanoscale, 2025, DOI: 10.1039/d4nr04131c**

# ELECTRONIC SUPPLEMENTARY INFORMATIONS (ESI †)

## The intriguing role of L-cysteine on the modulation of chiroplasmonic properties of chiral gold nano-arrows

Nada Khalfaoui Hassani,[a] Mary Tabut,[ab] Ndeye Haby Awe,[a] Christophe Desmarets,[c] Daniele Toffoli,[d] Mauro Stener,[d] Nicolas Goubet *[a] Monica Calatayud *[ab] and Caroline Salzemann *[a]

[a] *Sorbonne Université, MONARIS, CNRS-UMR 8233, 4 Place Jussieu, F-75005 Paris, France; E-mail: nicolas.goubet@sorbonne-universite.fr ; caroline.salzemann@sorbonne-universite.fr*

[b] *Sorbonne Université, CNRS, Laboratoire de Chimie Théorique, LCT, 4 Place Jussieu, F-75005 Paris, France; E-mail: monica.calatayud@sorbonne-universite.fr*

[c] *Sorbonne Université, IPCM, CNRS-UMR 8232, 4 Place Jussieu, F-75005 Paris, France*

[d] *Department of chemical and pharmaceutical sciences, University of Trieste, 34127, Trieste, Italy*

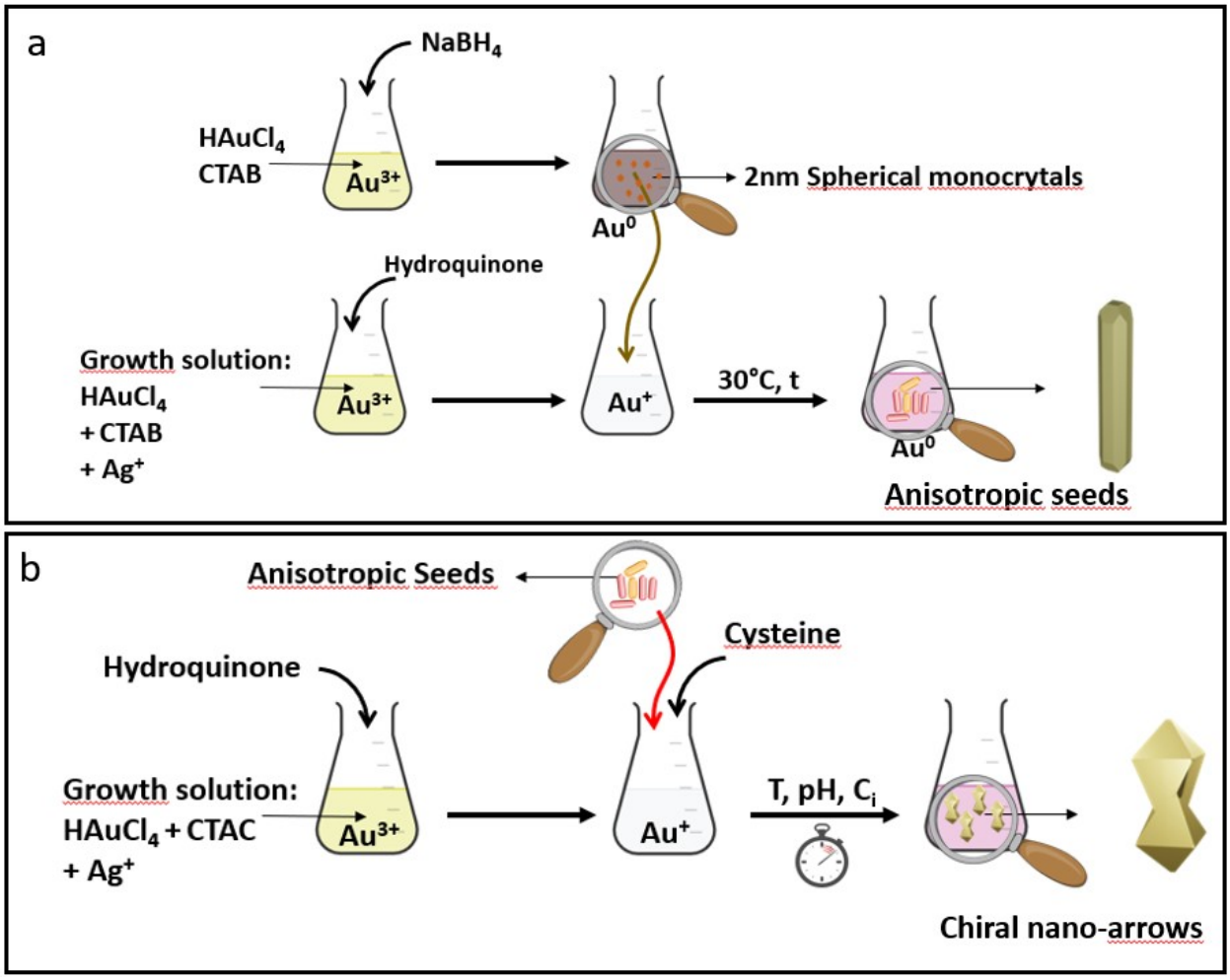


Fig. SI.1 Schematic representation of the synthesis by seeding process a) formation of nanorods seeds and b) their further growth to form nano-arrows.

This ESI replaces the original version published on 03 Jan 2025.

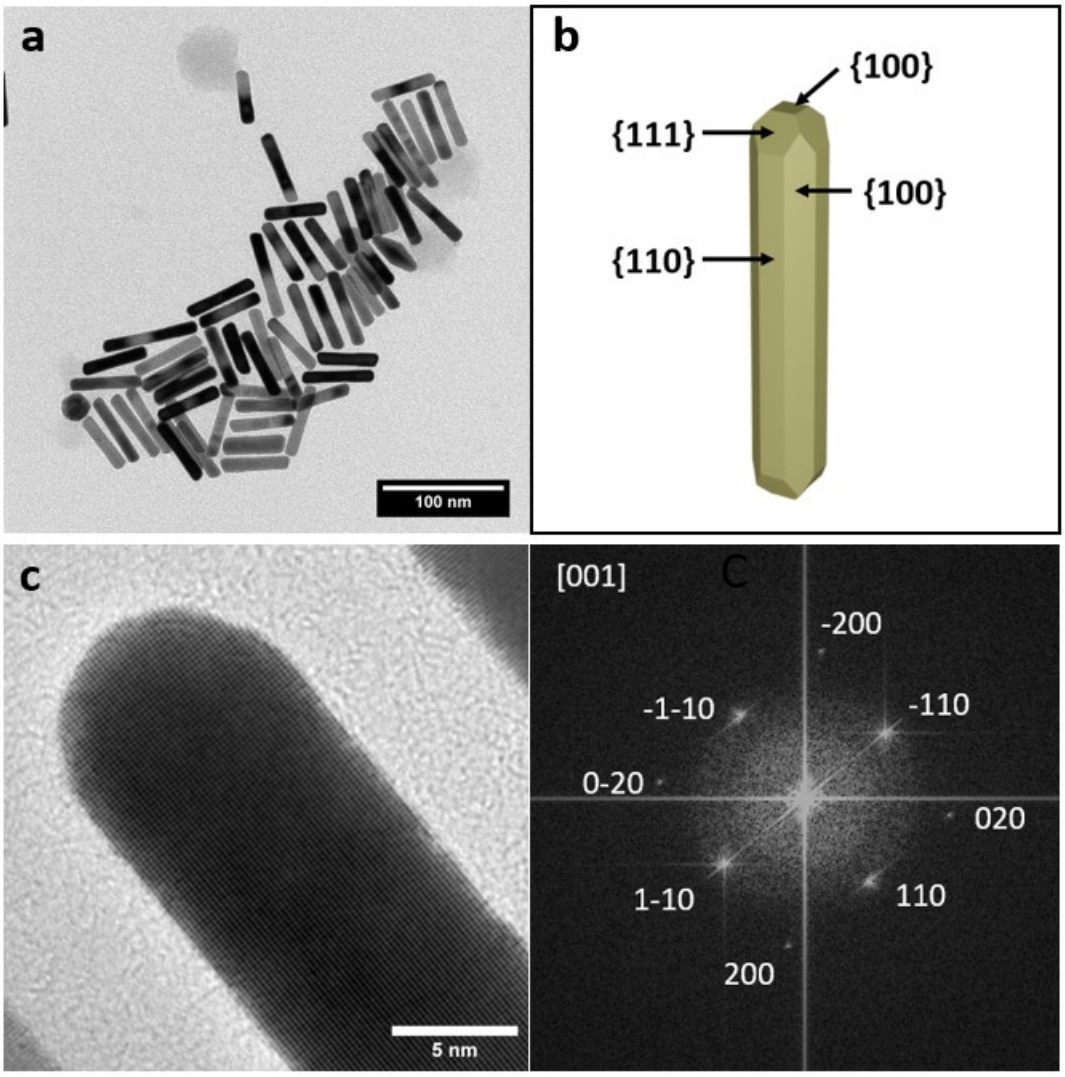


Fig. SI.2 Monocristalline gold nanorods obtained by seeding process with CTAB and hydroquinone. a) TEM image, b) schematic representation and c) HRTEM image and the corresponding calculated FFT.

This ESI replaces the original version published on 03 Jan 2025.

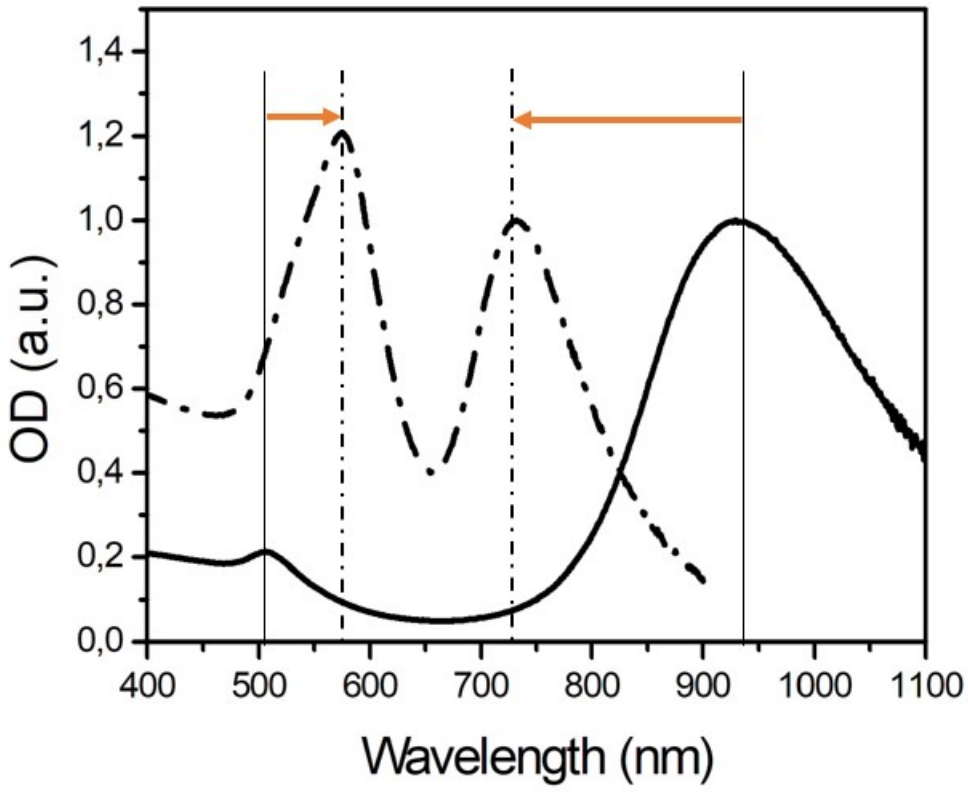


Fig. SI.3 UV-visible spectra of the elongated seeds (straight line) and of the nanoarrows in absence of cysteine (dash-point line).

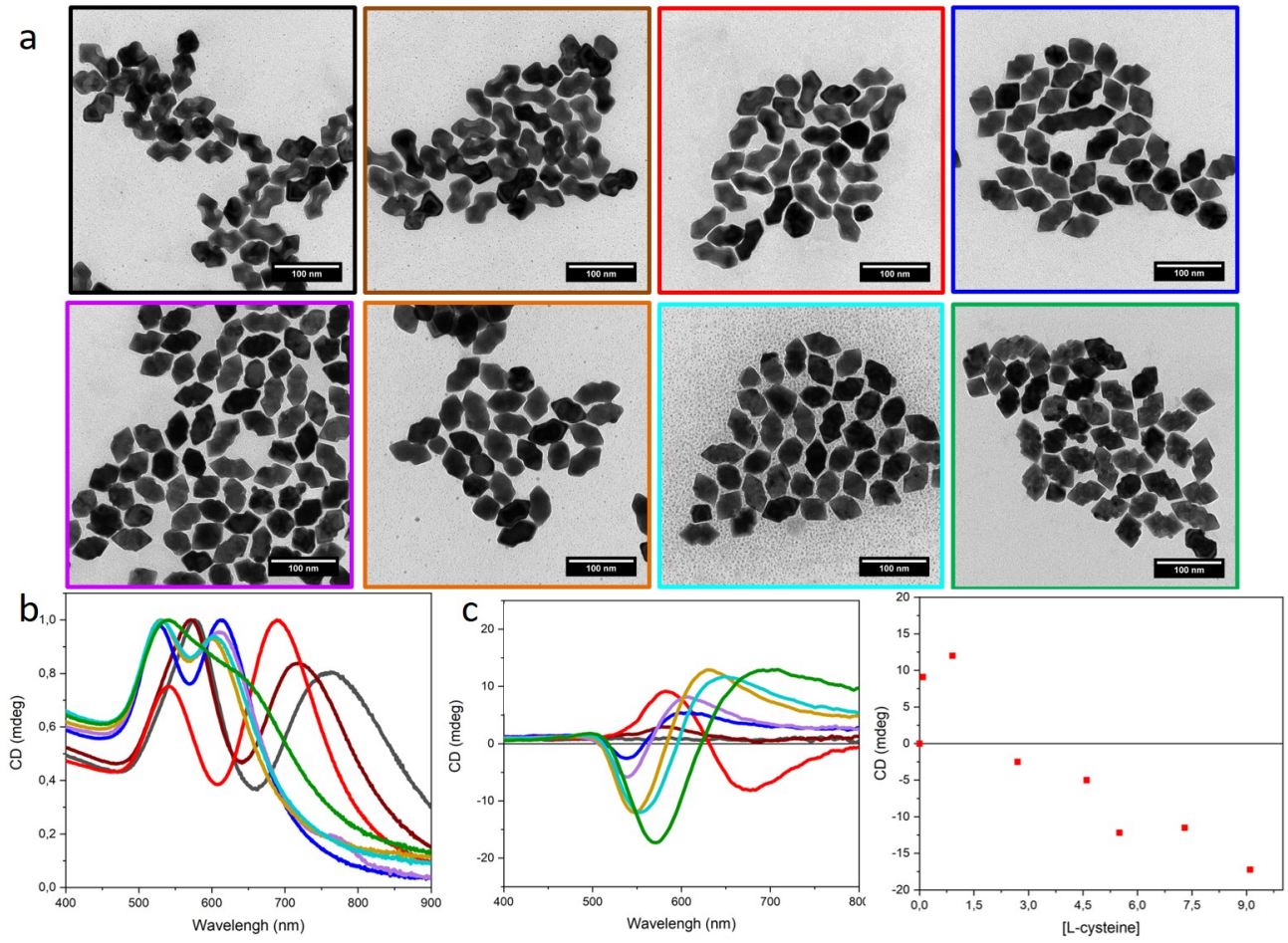


Fig. SI.4 TEM images (a), UV-visible absorption (b) and CD (c) spectra corresponding to nanoparticles obtained at 0 (black), 0.1 (red), 0.91 (dark blue), 2.7 (green) , 4.6 (violet), 5.5 (orange), 7.3 (light blue) and $9.1\,\mu\mathrm{mol}\mathrm{L}^{-1}$ of cysteine. d) Plot of the intensity of the first band of the corresponding CD signal.

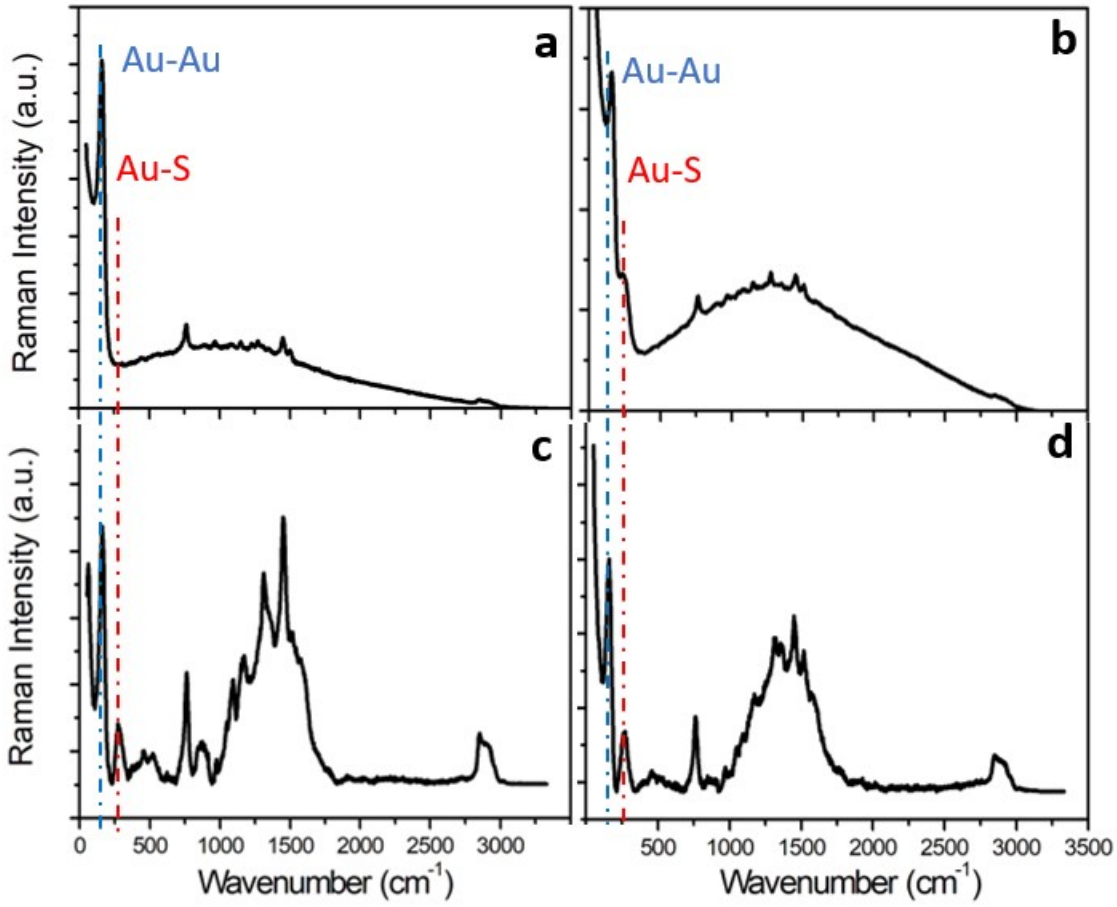


Fig. SI.5 Raman spectra for nano-arrows obtained a) in the absence of cysteine and with a concentration of b) $0.9\,\mu\mathrm{mol\,L^{-1}}$, c) $2.7\,\mu\mathrm{mol\,L^{-1}}$ and d) $9.1\,\mu\mathrm{mol\,L^{-1}}$.

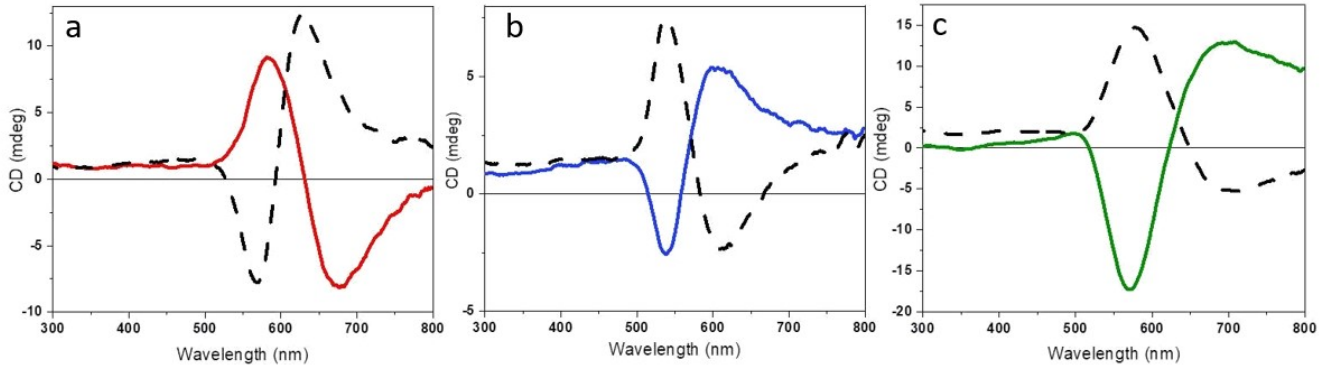


Fig. SI.6 Circular dichroism spectra obtained at a) $0.9\,\mu\mathrm{mol\,L^{-1}}$, b) $2.7\,\mu\mathrm{mol\,L^{-1}}$ and c) $9.1\,\mu\mathrm{mol\,L^{-1}}$ with L-cysteine (straigth line) and D-cysteine (dashed line)

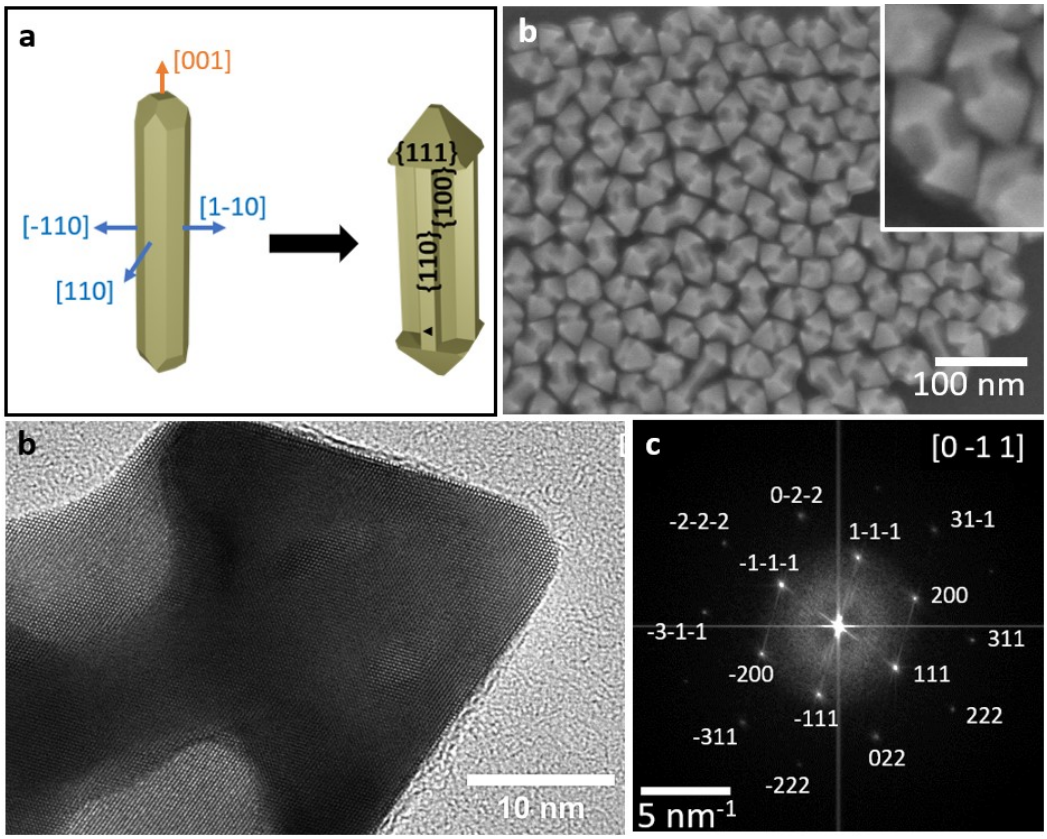


Fig. SI.7 a) schematic growth of nanoarrows from nanorods, b) SEM-FEG image of achiral nanoarrows obtained in absence of cysteine, c) HRTEM image and d) FFT calculated in the overall HRTEM image

| | Aspect ratio $AR = \frac{H + h_1 + h_2}{D}$ | Volume ($nm_3$) | Surface ($nm_2$) |
|---|---|---|---|
| 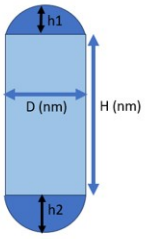  | $AR_{nanorods}$= | $V_{nanorod} = \pi H \left(\frac{D}{2}\right)^2 + \frac{\pi h_1^2}{3}\left[3\left(\frac{D}{2}\right) - h_1\right] + \frac{\pi h_2^2}{3}\left[3\left(\frac{D}{2}\right) - h_2\right]$ | $S_{nanorod} = \pi D(H + h_1 + h_2)$ |
| 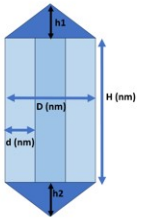  | $AR_{arrows}$=2.3 ± 0,3 | $V_{arrows} = H(D^2 - 4d^2) + (h_1 + h_2)\frac{D^2}{3}$<br>$V_{arrows}$ = (24 760.8 ± 3816) $nm^3$<br>$N_{at/NP}$= (1.46 ± 0.22) $10^6$ | $S_{arrows} = 2d\left[\sqrt{h_1^2 + \left(\frac{D}{2}\right)^2} + \sqrt{h_2^2 + \left(\frac{D}{2}\right)^2}\right] + 12dH$<br>$S_{arrows}$ = (5 861 ± 725) $nm^2$<br>$S_{110}$=40.2% and $S_{111}$=59.1% |

Fig. SI.8 Description of the nano-arrows and their volume and surface determinations.

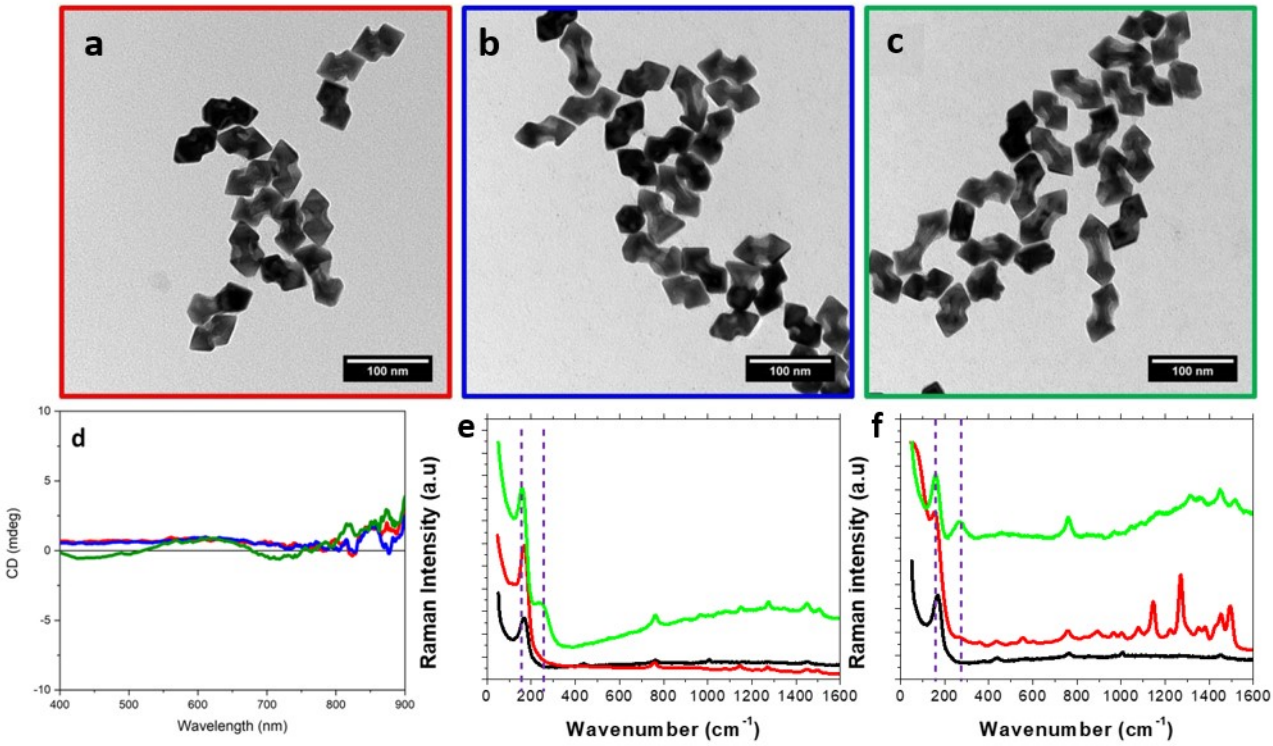


Fig. SI.9 TEM images of nanoarrows synthesized in absence of cysteine and keep after synthesis for 12 h in a) $0.9\,\mu\mathrm{mol\,L^{-1}}$, b) $2.7\,\mu\mathrm{mol\,L^{-1}}$ and c) $9.1\,\mu\mathrm{mol\,L^{-1}}$ of L-cysteine. d) the corresponding circular dichroism spectra. Raman spectra before (black) and after functionalization (red) in presence of e) $0.9\,\mu\mathrm{mol\,L^{-1}}$ and f) $9.1\,\mu\mathrm{mol\,L^{-1}}$ of cysteine. Green curves correspond to the Raman spectra of arrows growth in presence of cysteine (see Figure SI.5)

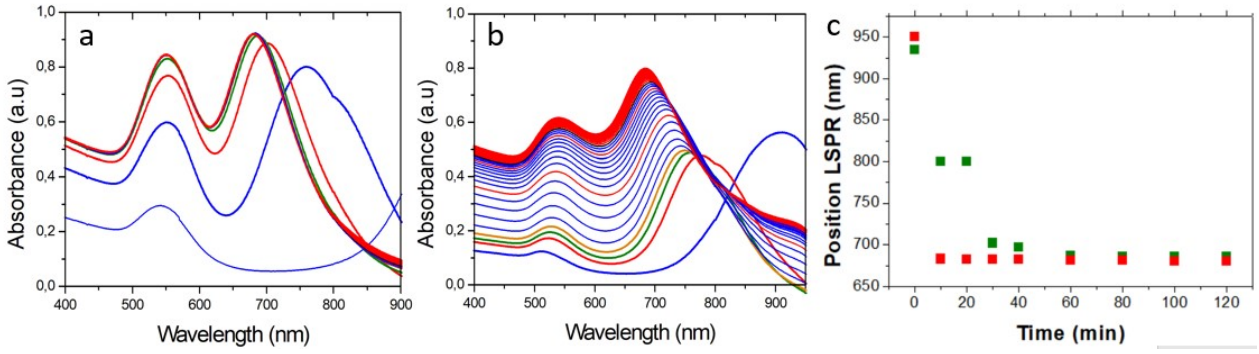


Fig. SI.10 UV-visible spectra monitored during the 240 min of reaction for a) $0.9\,\mu\mathrm{mol\,L^{-1}}$ and b) $9.1\,\mu\mathrm{mol\,L^{-1}}$ of L-cysteine. c) Plotted positions of the longitudinal-LSPR during the growth for $0.9\,\mu\mathrm{mol\,L^{-1}}$ (red) and $9.1\,\mu\mathrm{mol\,L^{-1}}$ (green) of L-cysteine.

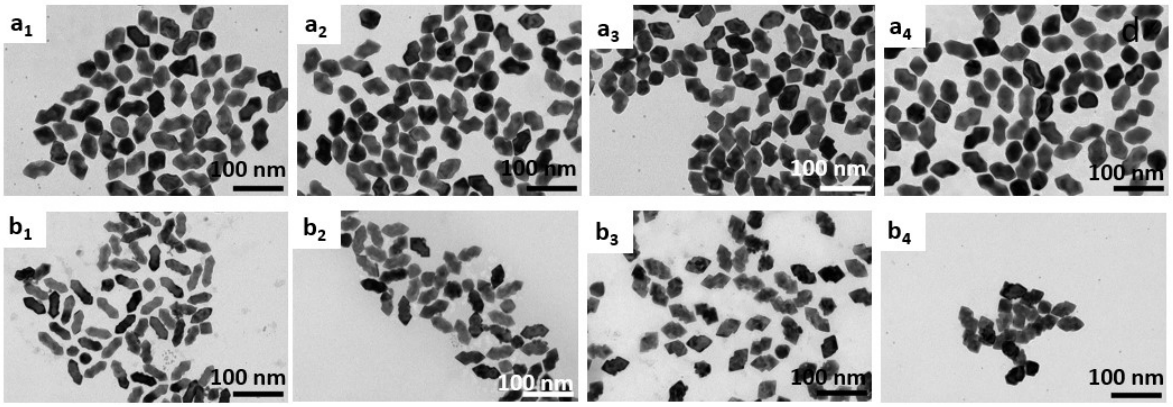


Fig. SI.11 : TEM images of extracted nanoparticles obtained in presence of $0.9\,\mu\mathrm{mol\,L^{-1}}$ (labeled $a_x$) and $9.1\,\mu\mathrm{mol\,L^{-1}}$ of cysteine (labeled $b_x$) at different time of reaction of 10 min (x=1), 30 min (x=2), 60 min (x=3) and 120 min (x=4).

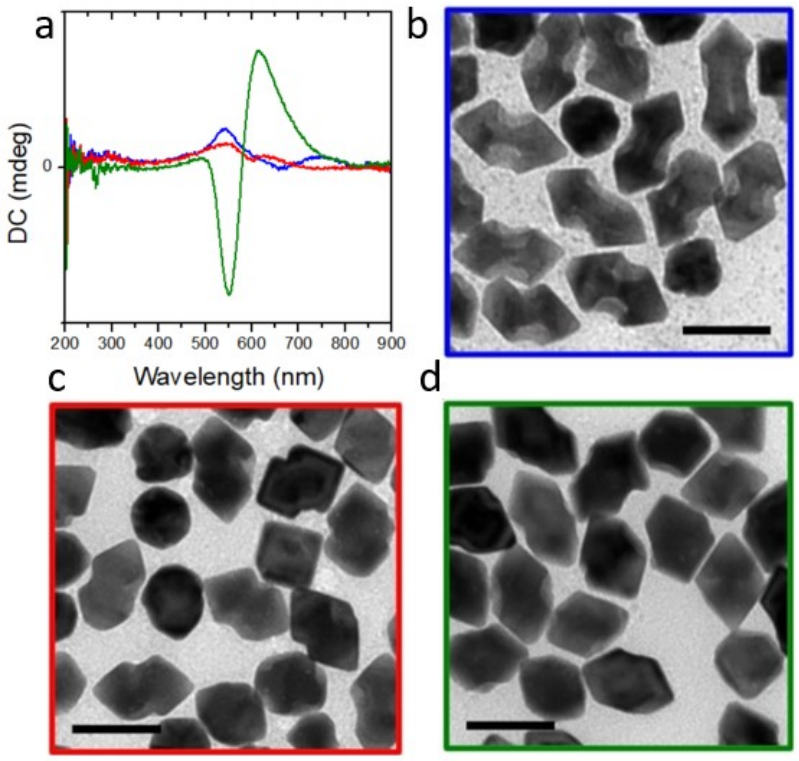


Fig. SI.12 CD spectra and TEM images of gold nanoparticles obtained in the presence of a) $0.9\,\mu\mathrm{mol\,L^{-1}}$ (blue), b) $2.7\,\mu\mathrm{mol\,L^{-1}}$ (red) and c) $9.1\,\mu\mathrm{mol\,L^{-1}}$ (green) of glutathione. The scale bare corresponds to 50 nm.

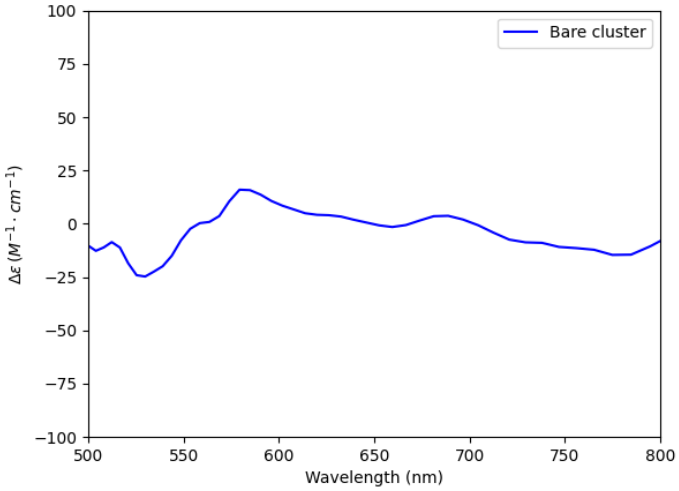


Fig. SI.13 Theoretical CD spectrum of the bare $Au_{64}$ cluster.